JOURNAL OF BACTERIOLOGY, Oct. 1985, p. 33–44
0021-9193/85/100033-12$02.00/0

Vol. 164, No. 1

Molecular and Genetic Analysis of the Transferred DNA Regions of the Root-Inducing Plasmid of *Agrobacterium rhizogenes*

FRANK F. WHITE,[1] BRIAN H. TAYLOR,[2] GARY A. HUFFMAN,[1] MILTON P. GORDON,[2] AND EUGENE W. NESTER[1]*

Department of Microbiology and Immunology[1] and Department of Biochemistry,[2] University of Washington, Seattle, Washington 98195

Received 11 March 1985/Accepted 19 June 1985

The T-DNA regions of the root-inducing (Ri) plasmid pRiA4b of *Agrobacterium rhizogenes* were characterized. Two regions, designated T_L-DNA and T_R-DNA, were found to be integrated and stably maintained in the plant genome. The T_L-DNA spanned a 15- to 20-kilobase region of pRiA4b and was separated from the T_R-DNA region by at least 15 kilobases of nonintegrated plasmid DNA. The T_R-DNA region also spanned a 15- to 20-kilobase region of pRiA4b and included a region of homology to the *tms* morphogenic loci of the tumor-inducing (Ti) plasmid of *Agrobacterium tumefaciens*. Eighteen deletions and 95 transposon insertions were generated in the T-DNA regions and tested for alterations in virulence. Insertions into four loci in the T_L-DNA affected the morphology of root formation of *Kalanchoë diagremontiana* leaves and stems, but had no visible effects on other host plants. Insertions into two loci (*tms-1* and *tms-2*) in the T_R-DNA eliminated virulence symptoms on all plants tested, with the exception of *K. diagremontiana* stems, where sparse root formation occurred. Complementation experiments with Ri and Ti plasmid T-DNA mutations indicate that the *tms* genes of the two plasmids serve similar functions and suggest a functional relationship between one or more genes of the T_L-DNA and the cytokinin synthesis locus *tmr* of the Ti plasmid.

Hairy root disease is caused by the soil bacterium *Agrobacterium rhizogenes* and is characterized by the extensive formation of adventitious roots at or near the site of infection. The ability of the bacterium to incite hairy root is encoded by a large plasmid called the root-inducing (Ri) plasmid (26, 41). The rhizogenicity of *A. rhizogenes* infections distinguishes hairy root tumors from the related disease, crown gall, which is incited by strains of *Agrobacterium* that harbor tumor-inducing (Ti) plasmids.

The underlying mechanisms for hairy root and crown gall tumorigenesis are likely to be very similar. In both cases, a portion of the Ri or Ti plasmid, called the T-DNA, is transferred to the plant cell, integrated into the host genome, and expressed as polyadenylated mRNA (11, 28). The T-DNA regions of two types of Ti plasmids (octopine and nopaline types) have been well characterized both genetically and physically (11, 28). The genes of the Ti plasmid T-DNA direct a variety of newly acquired phenotypic traits in the transformed plant cells, including the increased synthesis of two morphogenic phytohormones, auxin and cytokinin (2), and the synthesis of tumor-specific compounds called opines. Recent evidence has in fact demonstrated that the transcript 2 gene (designated *tms-2* here) is directly responsible for the production of the auxin indole-3-acetic acid from indole acetamide, which presumably is produced from tryptophan by the product of the *tms-1* gene (18, 33). The transcript 4 gene (designated *tmr* here) encodes an isopentyl transferase which supplies the intermediary compound isopentyl-5′-adenosine monophosphate in the cytokinin biosynthetic pathway (1, 3).

Ri plasmids have been isolated from a variety of strains and appear to fall within two classes, the mannopine and agropine types, based on the particular compounds that are synthesized by the transformed plant tissue (31). A comparison of the respective restriction fragment maps indicates that all agropine-type Ri plasmids examined are very similar and quite separate as a group from the mannopine-type plasmids (8, 9, 42). Several regions of DNA which may encode similar functions on Ri and Ti plasmids have been identified by hybridization studies (17, 24, 44). Both types of Ri plasmids share extensive homology with the Ti plasmids in the virulence (*vir*) region, which is a region of genes required for tumorigenicity and located outside the T-DNA (11, 28). The mannopine- and agropine-type Ri T-DNA regions both share sequence homology to the agropine synthesis loci of the octopine-type T-DNA and several genetically undefined regions of the nopaline-type T-DNA (17, 24, 44). The agropine-type Ri plasmids also contain homology to the two *tms* loci which are present in both nopaline- and octopine-type T-DNA (17, 44). No homology between Ri plasmid DNA and the *tmr* locus of the Ti plasmid T-DNA has been detected (17, 24, 44).

To further our understanding of the molecular basis of hairy root tumor induction, we have analyzed the T-DNA regions of the agropine-type Ri plasmid pRiA4b. A complete restriction map of pRiA4b has been recently constructed, and the regions of homology to the nopaline and octopine type Ti plasmids have been identified (17). In the present study, the portions of the Ri plasmid that were transferred to plant cells during tumor formation were determined. These T-DNA regions were then subjected to deletion and transposon mutagenesis to identify the contributions of each T-DNA region to the induction of hairy root disease. The results have revealed both an unusual organization of T-DNA functions and a novel set of morphogenic loci. A comparison of these results with previous studies on the T-DNA of Ti plasmids has afforded a better understanding of hairy root disease.

MATERIALS AND METHODS

Tumor lines. Tumor line A4-4a was initiated by stem inoculation of *Nicotiana glauca* with wild-type *A. rhizogenes*

* Corresponding author.

TABLE 1. Strains and plasmids

Strains and plasmids	Relevant phenotype or genotype[a]	Source
Agrobacterium spp.		
R1000 (pRiA4b)	Onc$^+$	Derivative of strain A4T (26)
R1150(pPH1JI)	Onc$^-$, Gn^r	R1000 cured of pRiA4b (this study)
A348(pTiA6NC)	Onc$^+$	(14)
A2100(pTiA6NC::NPT1)	*tms-2*, Kn^r (pUC4K)	(21)
A328(pTiA6NC::Tn*5-328*)	*tms-1*, Kn^r	(14)
A338(pTiA6NC::Tn*5-338*)	*tmr*, Kn^r	(14)
R1235(pRiA4b::Tmr$^+$)	Onc$^+$, Kn^r (Tn*5*)	pRiA4b containing *tmr* of pTiA6NC (this study)
R1236(pRiA4b 100::Tmr$^+$)	Onc$^+$ Kn^r (Tn*5*), Cb^r (Tn*3*)	R1200 with *tmr* of pTiA6NC (this study)
E. coli		
HB101	*thr leu thi pro*	
C2110	*polA gyrA*	(12)
2174(pPH1JI)	*met pro*, Gn^r, RK2^{rep}, IncP1	Obtained from J. Beringer
HB101rif(pRK2073)	Tra$^+$	(25)
Plasmids		
pVK102	Tc^r, Kn^r, λ Cos, RK2^{rep}, IncP1	(22)
pFW302	Tc^r, RK2^{rep}, IncP1	H-11 to H-18 of pRiA4b in pVK102 (this study)
pFW300	Tc^r, Cb^r, RK2^{rep}	H-11 to H-18 in pVK102/pHC79 (this study)
Col E1::Tn5	Kn^r	Obtained from D. Berg
pUC19	Cb^r	Cloning site of mp19 in pUC8 (38)
pUC4K	Kn^r, Cb^r	Contains NPTI gene (38)

[a] Cb^r, carbenicillin resistance; λCos, *cos* site of *E. coli* phage λ; Gn^r, gentamicin resistance; Kn^r, kanamycin resistance; *gyrA*, nalidixic acid resistance. (Origin of resistance gene is given in parentheses.) IncP1, plasmid incompatibility classification; RK2^{rep}, wide-host-range replication origin of pRK2; Tc^r, tetracycline resistance.

A4. Tumor line G5 was initiated on decapitated *N. glauca* with *A. rhizogenes* R1000. Explanted tumors were cultured as described previously (41).

Plant DNA isolation, fractionation, and hybridization. DNA from *N. glauca* was isolated by a modification of the procedure of Murray and Thompson (27). Plant DNA was digested with the appropriate restriction enzymes at 3 U/μg of DNA for 6 to 12 h under the conditions specified by the supplier (Bethesda Research Laboratories). The digested DNA was fractionated by electrophoresis (2.5 V/cm). Gels were washed for 1 h each in 0.5 N NaOH–0.8 M NaCl, 0.5 M Tris (pH 7.0)–1.5 M NaCl, and 20× SSC (1× SSC is 0.15 M NaCl, 0.015 M sodium citrate, pH 7.0) and transferred to nitrocellulose filters (35). Nitrocellulose filters containing bound DNA were baked at 80°C for 2 h and then prehybridized at 42°C overnight in 50% formamide–3× SSC–10 mM KH_2PO_4 (pH 6.5)–12.5 mM EDTA–5× Denhardt solution–0.5% sodium dodecyl sulfate–100 μg of denatured, sheared salmon sperm DNA per ml–5% dextran sulfate. Probes were ^{32}P labeled by nick translation, denatured by boiling, added to the prehybridization solution to give 2×10^6 cpm/ml, and incubated at 42°C for 24 to 48 h. The filters were washed in 2× SSC–2.5 mM EDTA–0.1% sodium dodecyl sulfate at room temperature for 10 min and twice at 65°C for 30 min and then twice in 0.3× SSC–2.5 mM EDTA–0.1% sodium dodecyl sulfate at 65°C for 30 min. Filters were autoradiographed on Kodak XAR-5 film with a Cronex Lightning Plus intensifying screen at −70°C for 2 to 7 days.

Reconstruction mixtures were prepared from mixes of salmon sperm DNA and pRiA4b plasmid DNA. The diploid molecular weight of the *N. glauca* genome is 4×10^{12} (13), and the ratio of the molecular weights of the *N. glauca* genome and pRiA4b (1.6×10^8) is 2.6×10^4. Therefore, 385 pg of pRiA4b was added to 10 μg of salmon sperm DNA (in place of *N. glauca* DNA) for a one-copy reconstruction mixture.

Bacterial strains and plasmids. *Agrobacterium* spp. and *Escherichia coli* strains and plasmids are listed in Table 1. R1000, the parent strain for subsequent mutations in the Ri plasmid, contains the 250-kilobase (kb) plasmid from *A. rhizogenes* A4T (26, 42). R1050(pPH1JI) was cured of pRiA4b by growth of the strain at high temperature (41).

Bacterial media. *Agrobacterium* strains were maintained on AB minimal agar (7) supplemented when appropriate with 100 μg of kanamycin (Sigma Chemical Co.) per ml, 200 μg of carbenicillin (Geopen; Pfizer Inc.) per ml, or 100 μg of gentamicin (Sigma) per ml. *E. coli* strains were maintained on L agar supplemented when appropriate with 50 μg of kanamycin per ml, 50 μg of carbenicillin per ml, 10 μg of tetracycline (Sigma) per ml, or 50 μg of nalidixic acid (Sigma) per ml. *E. coli* and *Agrobacterium* spp. matings were performed on nutrient agar (Difco Laboratories).

Bacterial plasmid isolation. The *Agrobacterium* spp. plasmid was prepared as previously described (41). *E. coli* clones were screened for plasmids by the rapid isolation procedure of Birnboim and Doly (4). Large quantities of cosmid or plasmid DNA were prepared from *E. coli* by a scale-up of this procedure (300 ml of culture was suspended in 10 ml of buffer) and purified by cesium chloride-ethidium bromide centrifugation. After extraction of the ethidium bromide, plasmid DNA was precipitated directly from the cesium chloride by the dropwise addition of 0.360 ml of cold ethanol per 0.5 ml of solution (or until cesium chloride began to precipitate).

Molecular cloning. Individual *Hin*dIII restriction fragments of the Ri plasmid T-DNA regions were subcloned from cosmid pFW22, pFW41, pFW55, or pFW94 into pHC79 (15). The clones were transformed to *E. coli* HB101. Transformants were selected for resistance to carbenicillin and then screened for sensitivity to tetracycline and for plasmid content.

Construction of pFW302 and pFW300. The T_L-DNA region of pRiA4b was recloned from pNW44 (17) by partial digestion and ligation into the mobilizable, wide-host-range cosmid vector pVK102 (22). The ligated DNA was packaged in vitro (22). Cosmid particles were transduced to *E. coli* C2110, and recombinant clones were selected for resistance to tetracycline. (The *polA* phenotype of C2110 does not

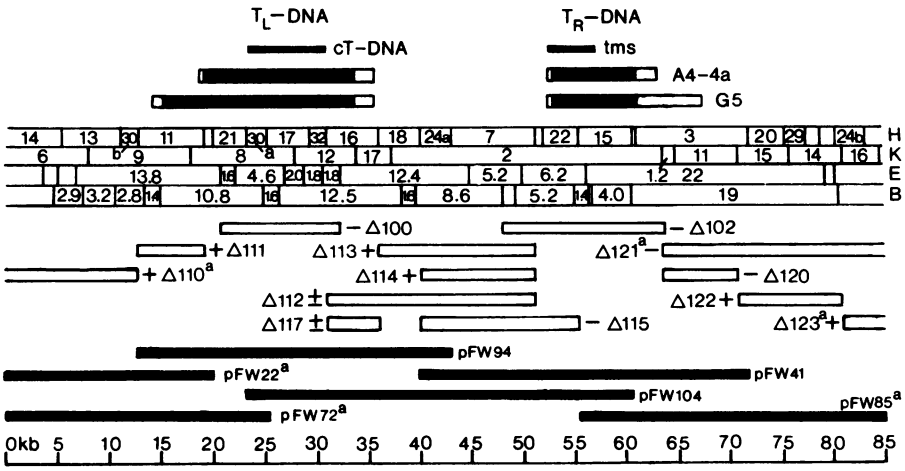

FIG. 1. Restriction map showing the locations of the T-DNA regions and the positions of deletions of pRiA4b. The fragment designations for *Hin*dIII (H) and *Kpn*I (K) are those assigned by Huffman et al. (17). The fragment designations for *Eco*RI (E) and *Bam*HI (B) are derived from the fragment size in kilobases. The unfilled portions of the bars indicate the approximate ends of the T-DNA regions. The open bars in the lower portion show the region of the Ri plasmid that is deleted in the strain. Virulence scores on *K. diagremontiana* leaves: +, wild-type response; ±, weak response; −, avirulent. The cosmid clones that were used in hybridization experiments and for deletion constructions are indicated by the solid bars at the bottom of the figure. The superscript a's indicate deletions and cosmid clones which extend to the right and left of the region depicted in the figure and were not shown in their entirety due to space considerations.

allow replication of pNW44, which contains the ColE1-type origin of replication.) Prospective clones were first screened for kanamycin sensitivity and subsequently characterized by restriction endonuclease analysis. The plasmid pFW302, which contained the same *Hin*dIII fragments of the T_L-DNA as contained in pFW94, was obtained by this procedure. Plasmid pFW300 also contained the same fragments as pFW94 and, in addition to the functions of pVK102, retained the gene for carbenicillin resistance from pHC79. The carbenicillin resistance gene provided a useful selective marker for introduction of pFW300 into *Agrobacterium* spp.

Bacterial conjugations and transformations. Nonmobilizable cosmids (pFW22, pFW94, pFW104, pFW41, and pFW85) were introduced into *Agrobacterium* spp. by the transformation procedure of Holsters et al. (16). Mobilizable plasmids (pFW302 and pFW300) in strain HB101 were introduced into *Agrobacterium* spp. by triparental matings (12) with the conjugation helper *E. coli* HB101rif(pRK2073) (25) on nutrient agar at 28°C overnight. Transconjugants were selected and purified on AB minimal agar (7) containing the appropriate antibiotics. Plasmid pPH1JI is a self-conjugal plasmid and was introduced into *Agrobacterium* spp. by mating on nutrient agar.

Deletion mutagenesis. Deletions were constructed from partial digests of cosmid clones of the pRiA4b T-DNA regions including pFW22, pFW41, pFW72, pFW94, pFW104 (17), and pFW85 (contiguous fragments H-15 to H-4 of pRiA4b in pHK17). Large partial digestion fragments were fractionated and purified by electroelution from agarose. The partially digested DNA was ligated to a 10-fold excess of phosphatase-treated restriction fragments which contain a gene conferring to an appropriate antibiotic resistance (2.5 U of calf thymus phosphatase [Boehringer Mannheim Biochemicals] per μg of DNA). ColE3::Tn*5*, which contains the kanamycin resistance gene on a single *Hin*dIII fragment (20), was used for *Hin*dIII deletions; linearized pUC19, containing the *bla* gene for carbenicillin resistance, was used for *Kpn*I deletions (38); and the single *Eco*RI fragment containing the kanamycin resistance gene from pUC4K (38) was used for *Eco*RI deletions. The ligated DNA was packaged into phage particles (22) and transduced to *E. coli* strain C2110. Clones were selected for resistance to tetracycline (cosmid vector gene) and the appropriate antibiotic. Clones were screened by restriction endonuclease analysis. The desired deletion mutations were introduced into pRiA4b by homologous recombination (14, 32), and the structure of the recombinants was verified by DNA hybridization.

Two strains were prepared by slight modifications of the above procedure. The deletion in R1200 was linked to Tn*3* (carbenicillin resistance) which had inserted within 0.5 kb of the deleted *Eco*RI fragments (Δ100, Fig. 1). Strain R1205 was constructed by deletion of the *Bam*HI fragments from pFW41::Tn*5-95*. The Tn*5* was oriented such that the kanamycin resistance gene of Tn*5* remained at the right end of the deleted *Bam*HI fragments (Δ102, Fig. 1).

Transposition mutagenesis. Tn*5* (kanamycin resistance) insertions were generated in infecting HB101 cells containing pFW72, pFW94, or pFW41 with Tn*5* as described by Ruvkun and Ausubel (32). Tn*3-HoHo1* (carbenicillin resistance) insertions were generated by a triparental mating between *E. coli* C2110 (*polA*) containing pFW302 (T_L-DNA cosmid), *E. coli* HB101 containing Tn*3-HoHo1* on pMB8, and *E. coli* HB101rif(pRK2073). The details of this procedure are described separately (Stachel et al., in press). The positions of the transposon were determined by restriction enzyme analysis with *Hin*dIII, *Bam*HI, and *Eco*RI. The insertion mutations were moved to pRiA4b by homologous recombination, and the resulting strains were verified by restriction analysis and DNA hybridization (14).

Introduction of pTiA6NC *tmr* gene. The *tmr* locus of pTiA6NC was cloned on a 6.8-kb *Sal*I fragment from pNW34D-2-1::Tn*5*-336 (14) into pUC8 (38). The *Sal*I *tmr* fragment was then cloned into the single *Xho*I site on the H-15 fragment of pRiA4b cloned in pHC79. The *Sal*I fragment, which contained the kanamycin resistance gene from Tn*5* and the *tmr* gene, was transferred to pRiA4b (strain R1000) and a deletion derivative of pRiA4b (strain R1200) by homologous recombination. The structures of the resulting strains, R1235 and R1236, respectively, were verified by hybridization (14).

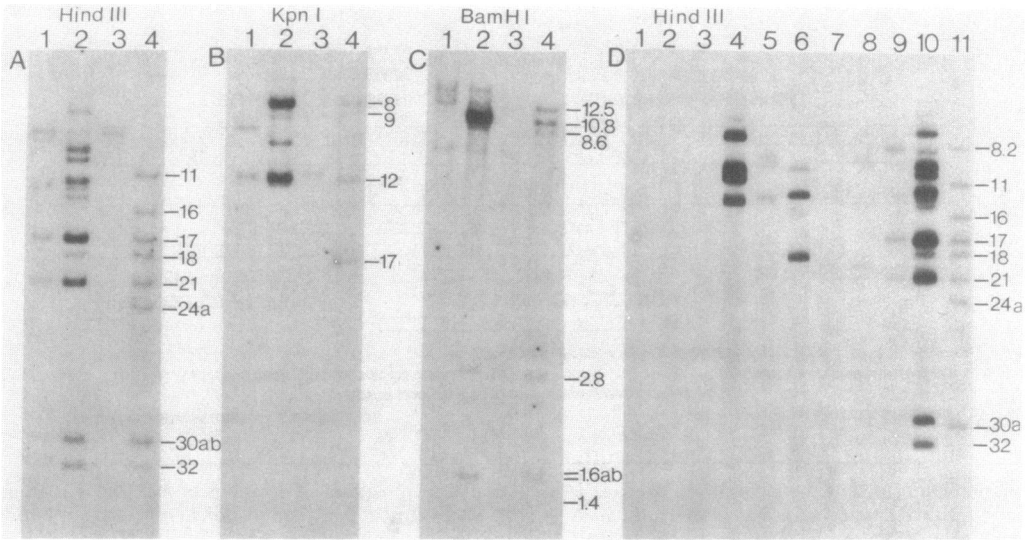

FIG. 2. Southern blot analysis of the T_L-DNA of pRiA4b. *N. glauca* tumor genomic DNA was fractionated and transferred to nitrocellulose. The DNAs for the filter hybridizations shown in A, B, C, and D were digested with *Hin*dIII, *Kpn*I, *Bam*HI, and *Hin*dIII, respectively. (A, B, C) Filters were hybridized with ^{32}P-labeled pFW94. Lanes: 1, A4-4a tumor DNA; 2, G5 tumor DNA; 3, normal *N. glauca* DNA; and 4, one-copy reconstruction in salmon sperm DNA. (D) Strip blots of A4-4a tumor DNA (lanes 1, 3, 5, 7, and 9) and G5 tumor DNA (lanes 2, 4, 6, 8, and 10) digested with *Hin*dIII and probed with the following ^{32}P-labeled plasmids: 1 and 2, H-30b; 3 and 4, H-11; 5 and 6, H-16; 7 and 8, H-18; 9, 10 and 11, pFW94. Lane 11 is a one-copy reconstruction in normal *N. glauca* DNA. The positions of the pRiA4b restriction fragments are indicated to the left of each autoradiograph. The 8.2-kb *Hin*dIII fragment observed in genomic digest of *N. glauca* DNA represents the region of homology to pRiA4b in the *N. glauca* genome.

Virulence tests. *Agrobacterium* strains were tested for virulence on at least four separate *Kalanchoë diagremontiana* plants (leaves and stems), and at least twice on tobacco stems (*Nicotiana tabacum* var *xanthi*), *N. glauca* stems, and carrot disks (*Daucus carota*) as described previously (41). Carrot disks are orientated such that the basal side of the root is up. All mutants containing pPH1JI were compared in virulence tests with R1000(pPH1JI) and an Ri plasmid-cured derivative, R1050(pPH1JI).

RESULTS

Two T-DNA regions of pRiA4b. Total genomic DNA from two *N. glauca* tumor lines, A4-4a and G5, was used to determine which regions of pRiA4b were present in transformed plant tissue. Genomic DNA was digested with restriction endonucleases, fractionated by gel electrophoresis, and transferred to nitrocellulose. The filter-bound tumor DNA was then hybridized to individual cosmid clones representing the entire pRiA4b plasmid. Three clones with overlapping segments of DNA, pFW22, pFW94, and pFW41 hybridized to DNA from both tumor lines (see Fig. 1 for regions covered by clones). All clones from other regions of pRiA4b that were used as probes were negative. Hybridization with pFW22 will not be considered further, since the hybridization obtained was subsequently found to be limited to a region of overlap between pFW22 and pFW94.

Both tumor lines contained *Hin*dIII fragments which hybridized to pFW94 and which comigrated with fragments H-21, H-30a, H-17, and H-32 (Fig. 2A, lanes 1, 2, and 4). The identity of these fragments was verified by hybridization with individual *Hin*dIII restriction fragments from pRiA4b (data not shown). T-DNA in cell line G5 extended into the left end of H-11 as indicated by the presence of the *Kpn*I fragment K-8 (Fig. 2B, lane 2) and the *Bam*HI fragment B-10.8 (Fig. 2C, lane 2), and presumably ended within the 1.4-kb *Bam*HI fragment in H-11, since this small *Bam*HI fragment was not detected (Fig. 2C, lane 2). No homology to the H-30b fragment, which is located to the left of H-11, was detected in either G5 or A4-4a (Fig. 2D, lanes 1 and 2). The A4-4a tumor DNA did not exhibit detectable hybridization to an H-11 probe (Fig. 2D, lane 3). Since H-21 was present in A4-4a (Fig. 2A, lane 1), the left end of the A4-4a T-DNA either included an undetectable portion of H-11 or extended only as far as the 0.8-kb *Hin*dIII fragment located between H-21 and H-11.

The T-DNA of G5 and A4-4a included sequences from the right of H-16, but did not contain the entire fragment (Fig. 2A, lanes 1 and 2). Both tumor lines contained a fragment that comigrated with the K-12 fragment (Fig. 2B, lanes 1 and 2). G5 also contained a fragment that comigrated with the H-18 fragment (Fig. 2A, lane 2), but no hybridization was detected to this fragment in either tumor line when H-18 was used as the probe (Fig. 2D, lanes 7 and 8). As observed in earlier studies, homology to DNA from untransformed plant tissue was detected in control experiments when pFW94 was the probe (Fig. 2, lanes 3A, 3B, and 3C).

Clone pFW41 overlaps the region of pRiA4b covered by pFW94 and includes *Hin*dIII fragments H-24a to H-3 (Fig. 1). When tumor DNA was probed with pFW41, the H-15 and B-4.0 fragments were found in both tumor lines (Fig. 3A, lanes 1 and 2, and Fig. 3C, lanes 1 and 2, respectively). Hybridization to tumor DNA was not observed when probed with H-7 (Fig. 3D, lanes 1 and 2) or H-24a (data not shown). G5 and A4-4a contained only a portion of H-22 as indicated by the absence of a fragment of corresponding size in either tumor line (Fig. 3D, lanes 3 and 4), thus placing the left extreme of this T-DNA region of pRiA4b in H-22. A fragment corresponding in size to H-3 was not detected in either tumor line (Fig. 3A, lanes 1 and 2), and no hybridization was detected to the adjacent fragment H-20 (Fig. 3D, lanes 7 and 8). The extent of the H-3 region of pRiA4b that was

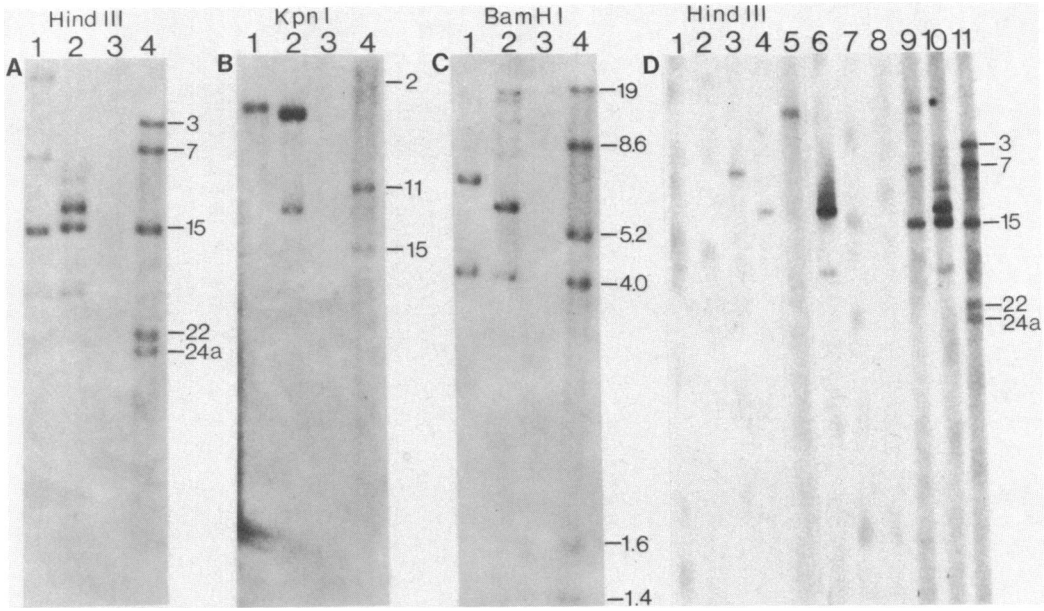

FIG. 3. Southern blot analysis of T_R-DNA of pRiA4b. *N. glauca* genomic DNA was fractionated and transferred to nitrocellulose. The DNAs for the filter hybridizations shown in A, B, C, and D were digested with *Hin*dIII, *Kpn*I, *Bam*HI, and *Hin*dIII, respectively. (A, B, C) Filters were hybridized with ^{32}P-labeled pFW41. Lanes: 1, A4-4a tumor DNA; 2, G5 tumor DNA; 3, normal *N. glauca* DNA; and 4, one-copy reconstruction. (D) Strip blots of A4-4a tumor DNA (lanes 1, 3, 5, 7, and 9) and G5 tumor DNA (lanes 2, 4, 6, 8, and 10) digested with *Hin*dIII and probed with the following ^{32}P-labeled plasmids: 1 and 2, H-7; 3 and 4, H-22; 5 and 6, H-3; 7 and 8, H-20; and 9 and 10, pFW41. Lane 11 is a one-copy reconstruction. The fragments were all cloned into pHC79. The positions of the pRiA4b restriction fragments are indicated to the left of each autoradiograph.

transferred and maintained in G5 and A4-4a was not clear from the data obtained. The T_R-DNA right border in A4-4a did not appear to span the K-1.2–K-11 junction since hybridization was observed to one single-copy *Kpn*I fragment (Fig. 3B, lane 1), nor has the K-1.2 fragment been detected by hybridization (data not shown). The right end of the T-DNA in G5 was represented on multiple *Kpn*I fragments (Fig. 3B, lane 2), and a fragment the size of the K-1.2 fragment has been observed (data not shown). Therefore, the T-DNA of the two tumor lines probably end at different positions in H-3. However, a more detailed analysis will be needed to determine the junction region. The hybridization to the *Hin*dIII-digested DNA indicated that the maximum size of fragments in G5 having homology with H-3 is 7 kb (Fig. 3D, lane 6).

The regions of pRiA4b that were detected in G5 and A4-4a are shown in Fig. 1. Although the exact organization of T-DNA in the tumors cannot be determined, these results established the two regions of pRiA4b that were transferred and maintained in the plant cells. These regions, hereafter referred to as the T_L-DNA (left T-DNA) and T_R-DNA (right T-DNA) regions, were separated by 16 kb of DNA (H-18, H-24a, H-7) that was not detected in the DNA of the transformed tumor lines.

Deletion analysis of T_L-DNA and T_R-DNA. To assess the contributions of each T-DNA region to virulence, deletions within and adjacent to the two T-DNA regions of pRiA4b were constructed (Fig. 1). In general, deletions were constructed by removing internal restriction fragments from cosmid clones covering the desired Ri plasmid regions by complete or partial restriction endonuclease digestion and replacing the deleted DNA with a DNA fragment containing an antibiotic resistance (Kn^r or Cb^r) gene. The deleted clone was checked by restriction endonuclease analysis, and the deletion was then transferred to the Ri plasmid in *Agrobacterium* spp. by homologous recombination. The fidelity of the marker exchange in *Agrobacterium* spp. was confirmed by hybridization analysis of total bacterial DNA with T-DNA region probes.

A strain harboring pRiA4b induced tumorigenic growth that included extensive root formation on both leaves and stems of *K. diagremontiana*. Root growth and the slight callus growth, which preceded root growth, were confined to the wound site (Fig. 4A). In addition, the roots tended to curl. Deletions that removed fragments of H-14 and H-13 (Δ110, Fig. 1) to the left of the T_L-DNA region or H-11, which is within the left border of the T_L-DNA (Δ111, Fig. 1), did not affect virulence. Removal of the core T_L-DNA region (Δ100, Fig. 1) altered the response to infection on *K. diagremontiana* leaves and stems, but had no effect on the response of other test plants (*N. glauca*, *N. tabacum*, *D. carota*). Δ100 prevented callus and root formation on *K. diagremontiana* leaves, whereas on stems, root formation, which is restricted to the wound site in the wild-type response, occurred along the stem (Fig. 4B). This root formation was accompanied by little or no callus formation at the wound site. The roots that did form did not have the curled appearance characteristic of roots resulting from infections with wild-type strains. Strains containing deletions that removed all or a portion of the sequences separating T_L-DNA and T_R-DNA incited wild-type symptoms, provided the deletions did not extend into the core regions of either T-DNA (Δ113 and Δ114, Fig. 1). A deletion that removed the nonintegrated inter-T-DNA region and fragment H-16 (Δ112, Fig. 1), which comprised the right end of the T_L-DNA, resulted in a weakened virulence response, since fewer roots were consistently observed on *K. diagremontiana* leaves compared with the wild type strain (data not shown). A similar response was seen when H-16 was deleted (Δ117, Fig. 1). However, in both cases the

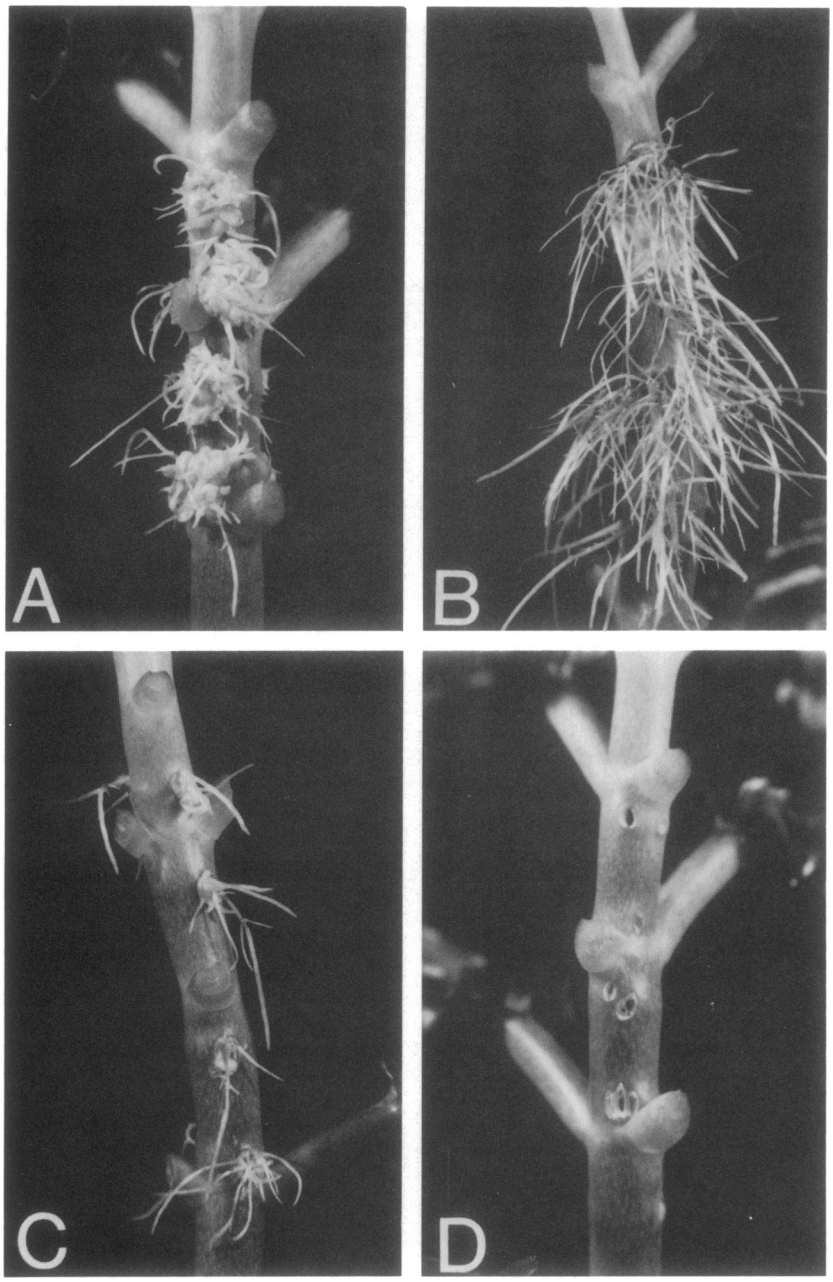

FIG. 4. Effects of pRiA4b T-DNA deletions on hairy root tumor morphology on *K. diagremontiana* stems. Hairy root tumors 1 month after inoculation of stems with the following: (A) R1000(pPH1JI); (B) R1200, T_L-DNA deletion (Δ100, Fig. 1); (C) R1205, T_R-DNA deletion (Δ102, Fig. 1); or (D) R1240, T_L-DNA and T_R-DNA deletions (Δ100 and Δ102, Fig. 1).

morphology of the rooting response did not appear to be affected.

Two strains harbored deletions that removed core T_R-DNA sequence, including part or all of the region containing the homology to the Ti plasmid *tms* genes. Δ115 deleted the fragments separating the T-DNA regions and the H-22 fragment from within the T_R-DNA. Δ102 removed most, if not all, of the T_R-DNA. Strains with Δ115 or Δ102 did not induce callus or root growth on any of the plants (including *K. diagremontiana* leaves) tested, with the exception of *K. diagremontiana* stems, where the mutant strains were still capable of inducing sparse root growth from the wound site (Fig. 4C). A similar effect on virulence was observed for deletion strains lacking sequences within or near the right border of the T_R-DNA. Deletion of K-1.2, K-11, and adjacent *Kpn*I fragments (Δ121, Fig. 1) or just the deletion of K-1.2 and K-11 (Δ120, Fig. 1) resulted in strains that were avirulent on all plants, with the exception of sparse root formation on *K. diagremontiana* stems.

Deletions in either T-DNA alone did not completely eliminate root formation on *K. diagremontiana* stems. The root-inductive properties of strains containing only one T-DNA region were proven to reside on the remaining T-DNA sequences by deleting both T-DNA regions from one strain. A strain with both deletions was constructed by incorporating deletion Δ102 into a strain containing Δ100.

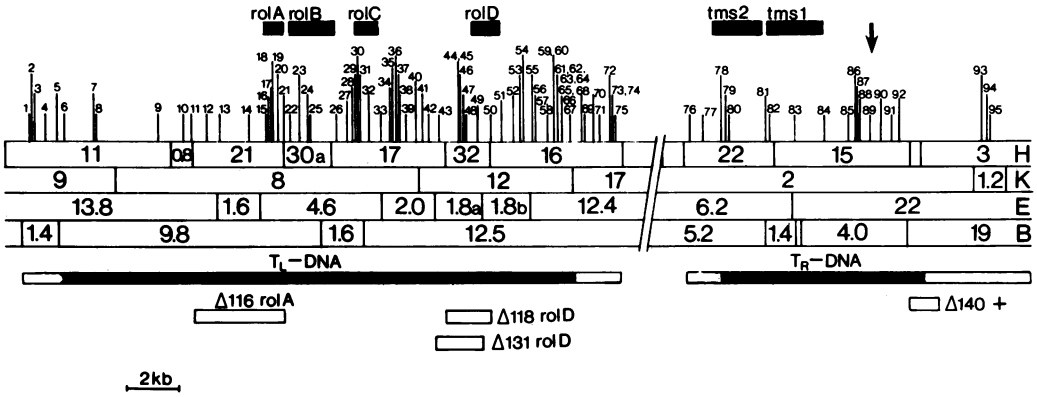

FIG. 5. Positions of transposon insertions and deletions into T_L-DNA and T_R-DNA regions of pRiA4b. The position of each insertion is indicated by a vertical line. The solid boxes in the upper portion indicate morphogenic loci (*rolA*, *rolB*, *rolC*, *rolD*, *tms-1*, and *tms-2*) and are extended to the nearest phenotypically silent insertion. The map region between the T_L-DNA and T_R-DNA regions was excluded from the figure. Deletions are indicated by the open boxes along with the virulence phenotype as assayed on *K. diagremontiana* leaves. The arrow designates the position of the *Xho*I site in H-15 and where the *tmr* gene was inserted. Restriction enzyme sites: H, *Hin*dIII; K, *Kpn*I; E, *Eco*RI; and B, *Bam*HI.

This strain (R1240) did not induce root formation on *K. diagremontiana* stems (Fig. 4D). Therefore, both T-DNA regions of pRiA4b contained loci that promoted root development. The functions of the T_L-DNA were not required for tumorigenesis on most of the host plants, and were essential only for callus and root formation on *K. diagremontiana* leaves. On all test plants, with the exception of *K. diagremontiana* stems, the T_R-DNA region of pRiA4b was essential for hairy root tumorigenesis.

Insertion analysis of the left and right T-DNA regions. Transposon insertion mutations and a number of small deletions were introduced into the two T-DNA regions to identify specific genetic loci involved in tumorigenicity (Fig. 5). Sixty-one Tn*5* and 34 Tn*HoHo* insertions were generated

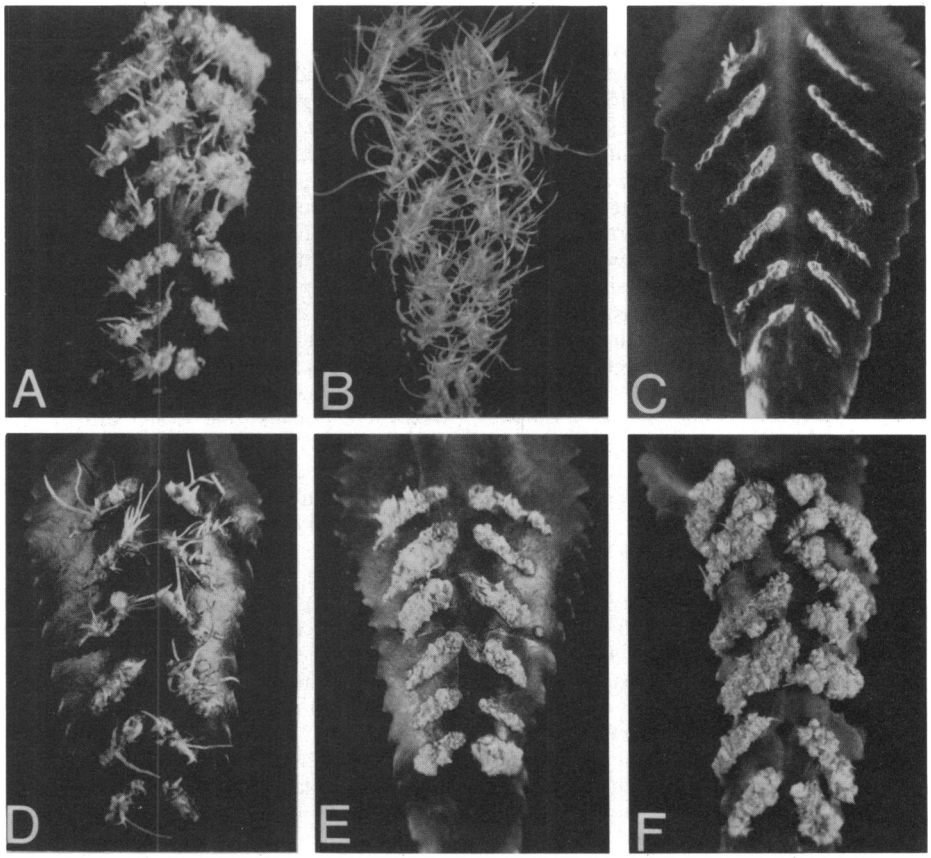

FIG. 6. Effects of mutations of the T_L-DNA *rol* loci of pRiA4b. Hairy root tumors one month after inoculation of *K. diagremontiana* leaves with (A) R1000(pPH1JI) (wild type), (B) R1022 (insertion 18, *rolA*), (C) R1023 (insertion 24, *rolB*), (D) R1020 (insertion 27, weakly virulent, no *rol* locus assigned), (E) R1016 (insertion 30, *rolC*), and (F) R1224 (Δ118, *rolD*). Refer to Fig. 5 for the positions of the mutations on pRiA4b.

in clones covering the T_L-DNA and T_R-DNA regions. These insertions were mapped, introduced into pRiA4b in *Agrobacterium* spp., and tested for the effects of the mutations on virulence. Several small deletions were generated in vitro and processed in a similar manner. The mutant bacterial strains were screened initially on *K. diagremontiana* leaves since this plant was particularly sensitive to alterations in both T-DNA regions.

The wild-type symptoms of infection on *K. diagremontiana* leaves involved first a slight formation of callus growth, followed by abundant root formation (Fig. 6A). The roots' tendency to curl and the fact that the response was restricted to the immediate vicinity of the wound gave the tumors a compact appearance. The mutations in the T_L-DNA defined at least four genetic loci that resulted in variant tumor phenotypes and that were given the tentative designations of *rolA*, *rolB*, *rolC*, and *rolD* (root locus; Fig. 5). Six strains containing Tn*5* insertions in the right end of H-21 defined the *rolA* locus. The roots induced by *rolA* mutants grew straight and away from the plant surface, resulting in an extra rooty appearance when compared with the wild-type hairy root symptoms (Fig. 6B). To cover regions of H-21 that were not mutated by insertion, the entire fragment was deleted. The strain with this deletion (Δ116, Fig. 5) incited tumors with phenotypes similar to the *rolA* insertions. If there were additional loci in H-21, then the phenotypes were masked by the *rolA* phenotype. Four strains with Tn*5* insertions which mapped within H-30a (*rolB*, Fig. 5) resulted in an avirulent response on *K. diagremontiana* leaves (Fig. 6C). No phenotypically wild-type insertions separated *rolA* from *rolB*. The *rolA* locus probably extended into H-30a, since an insertion of the *Hin*dIII fragment of Tn*5* at the H-21–H-30a junction created a strain with the *rolA* phenotype (insertion 21, Fig. 5).

Insertions in four strains at a third T-DNA locus, *rolC*, resulted in attenuated root growth from wound sites on *K. diagremontiana* leaves. A slight callus growth occurred at the wound site, as would occur in the wild-type infection before root emergence, but subsequent root growth was retarded (Fig. 6E). Insertions between *rolB* and *rolC* did not eliminate or attenuate root growth on *K. diagremontiana* leaves. However, several of these strains consistently induced less callus and root growth on *K. diagremontiana* leaves when compared with inoculations with wild-type strains on the same plant (Fig. 6D). The degree of the weakened response varied among the mutants in this region and between inoculations. Another genetic locus might therefore lie between *rolB* and *rolC*. However, a locus was not assigned to this region due to the varied response of the different mutants. Alternatively, the insertions may have affected the expression of the adjacent loci.

The *rolD* locus was defined by two insertions (insertions 49 and 50, Fig. 5) and two short deletions (Δ131 and Δ118, Fig. 5) which removed fragments E-1.8a and H-32, respectively. These mutations resulted in an increased formation of callus (Fig. 6F). Root initiation still occurred, but subsequent root growth was retarded. The location of *rolD* is somewhat ambiguous. Insertion 50 mapped just within the H-16 fragment, indicating that *rolD* was at the right end of H-32 and just spanned the H-32–H-16 junction. However, deletion of H-16 (Δ117, Fig. 1) did not result in the accentuated callus formation phenotype, but resulted in an overall weakened response as discussed above. An additional 18 insertions between *rolC* and *rolD* and 25 insertions beyond *rolD* were phenotypically wild type.

Two loci, which by DNA homology appear to correspond to the *tms* genes of the Ti plasmids, were identified in the T_R-DNA by insertion mutagenesis. Mutations in either locus resulted in an avirulent phenotype on *K. diagremontiana* leaves, *N. glauca* stems, and *N. tabacum* stems. The two strains with *tms-1* insertions (insertions 82 and 83; Fig. 5) were avirulent on carrot (*D. carota*) disks, whereas the three *tms-2* mutants (insertions 78, 79, and 80; Fig. 5) were weakly virulent. Mutations in *tms-1* or *tms-2* allowed sparse root formation on *K. diagremontiana* stems (see response of T_R-DNA deletion, Fig. 4C). One insertion with a wild-type phenotype separated the *tms* loci (insertion 81, Fig. 5). Twelve Tn*5* insertions and one short deletion (Δ140, Fig. 5) within a 7-kb region to the right of *tms-1* resulted in wild-type responses.

Complementation of Ri and Ti T-DNA genes. The mutagenesis of the T_R-DNA region of the Ri plasmid along with the earlier homology studies suggested that this region most likely contains functional homologs to *tms-1* and *tms-2*. A direct comparison of these genes was made by complementing the functions of mutated copies with the wild-type copies in the respective Ri or Ti plasmid. Complementation of the *tms* genes was tested by coinoculating plants with a mixture of two strains, each containing mutations in its respective Ri or Ti *tms* genes. This approach has been demonstrated to be an effective test of complementation in several studies (18, 30). Mutations in *tms-1* or *tms-2* in either pRiA4b or pTiA6NC, respectively, resulted in weak tumor responses on *K. diagremontiana* stems and leaves (Fig. 7A and B, respectively). A mixed infection with an Ri *tms-1* mutant (R1149) and a Ti *tms-2* mutant (A2100) or with an Ri *tms-2* mutant (R1132) and a Ti *tms-1* mutant (A328) resulted in a strong tumor response (Fig. 7C). A mixed infection with strains carrying Ri and Ti plasmids each with an insertion in the *tms-2* gene and each with an insertion in the *tms-1* gene, respectively, produced only a weak response on *K. diagremontiana* stems and leaves (Table 2).

There were no data suggesting a structural relationship between the genes of the Ri plasmid T_L-DNA loci and any known Ti plasmid T-DNA loci. However, the Ri T_L-DNA could functionally complement a mutation in the *tmr* locus of pTiA6NC. The complementation was performed after the interesting observation was made that the T_L-DNA deletion in pRiA4b (Δ100, Fig. 1) caused a tumor phenotype that was similar to the tumor phenotype of a Ti plasmid *tmr* mutant strain (A338). Both R1200 and A338 induced little observable tissue growth on *K. diagremontiana* leaves and caused stem wound responses that were indistinguishable from each other (Fig. 7D and E, respectively). The ability to form tumors on *K. diagremontiana* leaves and stems was restored to A338 when it was coinoculated with strain R1205 (Δ102, Fig.1), which contained an intact Ri T_L-DNA, but not with R1200 (Δ100, Fig. 1), which was deleted for the T_L-DNA region (Table 2). When the Ri plasmid T_L-DNA was provided directly in A338 in a *trans* configuration on clone pFW300, the resulting strain was tumorigenic. Root initiation along the stem was inhibited, and callus unaccompanied by roots formed at the wound site (Fig. 7F). Tumor formation was also restored on *K. diagremontiana* leaves (Table 2).

In the reverse experiment, the *tmr* gene was introduced into the Ri plasmid (arrow, Fig. 5). Root formation on *K. diagremontiana* stems caused by R1200 (Δ100, Fig. 1) was inhibited (response similar to phenotype shown in Fig. 7F), and tumor formation on *K. diagremontiana* leaves was restored. However, in this case the callus growths produced numerous shoots similar to the teratoma phenotype obtained

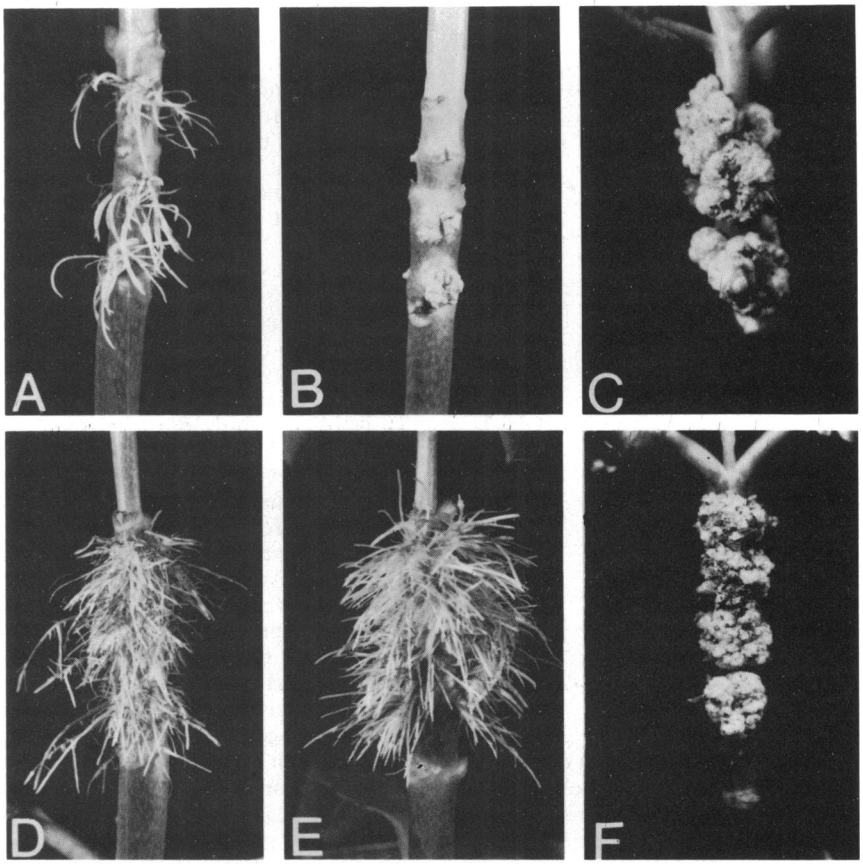

FIG. 7. Comparison of Ri and Ti plasmid T-DNA loci. Tumors 45 days after inoculation of *K. diagremontiana* stems with the following strains or mixture of strains (relevant mutation described in parentheses): (A) R1149 (Ri *tms-1*), (B) A2100 (Ti *tms-2*), (C) R1149 and A2100, (D) R1200 (pRiA4b T_L-DNA deletion), (E) A338 (Ti *tmr*), and (F) A338(pFW300). Cosmid pFW300 contains the entire T_L-DNA region of pRiA4b. The sources of the strains are listed in Table 2.

with some Ti plasmid-containing strains (Fig. 8A). Interestingly, when the Ri plasmid T_L-DNA was left intact and the *tmr* locus was added, tumors resulted that produced both leaves and roots, a phenotype not previously observed in either wild-type or mutant strains of *Agrobacterium* (Fig. 8B).

DISCUSSION

This study has identified T-DNA components of pRiA4b involved in hairy root tumorigenesis. The results also demonstrate an interesting feature of pRiA4b. In contrast to Ti plasmids, where the oncogenic genes are tightly linked (14, 18), the morphogenic functions of pRiA4b are divided between two widely separated T-DNA regions. These regions each cover at least 15 kb of pRiA4b and are separated from each other by approximately 16 kb of nonintegrated DNA.

The reason for the T-DNA organization of pRiA4b is unknown, but the arrangement probably reflects the evolutionary history of the plasmid. The wide-host-range octopine-type Ti plasmid pTiA6NC also contains a second T-DNA (36) which encodes the genes for mannopine and agropine synthesis (10), and two T-DNA regions have recently been found in limited-host-range Ti plasmids (5, 45). One possibility is that regions of T-DNA reflect adaptations to particular host plants, and multiple T-DNA regions may reflect further adaption to new hosts by combining individual T-DNA regions in one strain.

The deletions of the Ri T-DNA border regions suggest that each region may be bounded by sequences found in Ti plasmid T-DNA regions, which recent evidence indicates play critical roles in the efficient transfer or integration of the T-DNA to the plant genome (34, 39). Deletion of the right border of either Ri plasmid T-DNA region appears to affect virulence. Deletions of the right side of the T_R-DNA region have particularly dramatic effects. Such mutations have the same effect as removing the *tms* loci and are avirulent on all plants, with the exception of sparse root formation on *K. diagremontiana* stems. Similar effects are observed when the right border of the nopaline-type and octopine-type T-DNA is deleted (19, 23). The deletion of the Ri T_L-DNA appears to be less severe on oncogenesis than the T_R-DNA deletions. The deletions probably affect the *rolD* locus, but they do not have simply the *rolD* phenotype. It is possible that these strains incite a weakened response due to a combination of a *rolD* mutation and reduced transfer of the T_L-DNA sequences, which is perhaps mediated by the T_R-DNA right border. Deletions of the left border region of the T_L-DNA have no apparent affect on oncogenesis.

The T_R-DNA is the T-DNA component of pRiA4b most comparable to the T-DNA of Ti plasmids. Homology, mutagenesis, and complementation experiments all indicate that the two morphogenic loci of the T_R-DNA correspond to the *tms* loci of the Ti plasmids, and that the *tms* genes play critical roles in hairy root tumorigenesis. The tumorous growth of plant cells after Ti plasmid transformation results from the increased synthesis of auxin and cytokinin directed

TABLE 2. Comparison of Ri and Ti plasmid T-DNA functions

Strain (relevant genotype or phenotype)	Virulence on *K. diagremontiana*[a]	
	Leaves	Stems
R1000 (wild-type hairy root)	+	+
A348 (wild-type crown gall)	+	+
R1132 (Ri plasmid *tms-1*)	−	±
R1149 (Ri plasmid *tms-2*)	−	±
A328 (Ti plasmid *tms-1*)	±	±
A2100 (Ti plasmid *tms-2*)	±	±
R1132 + A328	±	±
R1149 + A2100	±	±
R1132 + A2100	+	+
R1149 + A328	+	+
R1205 (Ri *tms-1* and *tms-2* deletion)	−	±
R1200 (Ri T_L-DNA deletion)	−	±[b]
A338 (Ti *tmr*)	−	±[b]
R1200 + A338	−	±[b]
R1205 + A338	+	+
A338(pFW300) (Ti *tmr* + Ri T_L-DNA)	+	+
R1235 (pRiA4b::*tmr*$^+$)	+[c]	+[c]
R1236 (pRiA4b100::*tmr*$^+$)	+[d]	+[d]

[a] Virulence scores indicate readily discernible plant tissue growth: +, extensive callus or root growth from wound; ±, sparse callus or root growth; −, little or no callus or root growth.
[b] Extensive root formation along stem.
[c] Tumors with shoots and roots.
[d] Tumors with shoots.

by the products of the T-DNA *tms-1*, *tms-2*, and *tmr* genes, respectively (1, 3, 33). Mutations in the *tms* genes of the Ti plasmid do not eliminate tumorigenic symptoms on most plants, although the mutations do alter considerably the morphology of the tumors (14, 19, 29). The tissue proliferation of the Ti plasmid *tms* mutants is attributable to the *tmr* gene, and only upon inactivation of both *tms* and *tmr* genes does a strain cause little or no tissue proliferation (28). The *tms* genes of the T_R-DNA of pRiA4b are likely also to provide for auxin synthesis in hairy root tumors, although we have not tested this directly. Removal or inactivation of either Ri *tms* gene has a drastic effect on virulence, rendering the strain essentially avirulent on most plants tested in this study. For these plants, root proliferation (and callus growth in the case of *N. glauca*) appears to be primarily due to the action of the *tms* genes, and in these circumstances, the Ri plasmid functions in a manner similar to a Ti plasmid containing a mutation in the *tmr* gene.

The T_L-DNA region is perhaps the most interesting region of the Ri plasmid. We have previously reported that this region shares homology with sequences already present in the uninfected *N. glauca* genome (40). The lack of homology within the four loci identified in this study to any Ti plasmid T-DNA genes (17) now suggests that the Ri T_L-DNA contains a novel set of morphogenic genes (although comparisons of homology at the level of the amino acid sequence await DNA sequencing data). The four T_L-DNA loci were assigned on the basis of the mutant phenotypes. Whether all of these loci are, in fact, separate genetic loci remains to be determined. In particular, *rolA* and *rolB* are not separated by phenotypically silent transposon insertions. Thus, we cannot exclude the possibility that the different phenotypic effects of mutations at *rolA* and *rolB* are the result of insertions into different regions of a single locus. Alternatively, more than one transcript may be encoded at any of the loci, as was found for the original *tms* mutations of the Ti plasmid (14). However, transcription studies have only associated one transcript with each locus (B. Taylor, Ph.D. thesis, University of Washington, 1984).

Costantino et al. (9) have determined that at least one T-DNA segment is maintained in *N. tabacum* transformed with the agropine-type Ri plasmid pRi1855. This T-DNA corresponds to the T_L-DNA of our study. We have detected an additional T-DNA region which, by a comparison of the restriction maps of the two plasmids, is also present on pRi1855. The possibility exists that some portion of T_R-DNA may also be found in these transformants, since their analysis did not extend into the T_R-DNA region. Costantino et al. (9) also reported that several of their transformants synthesized agropine. Genes involved in agropine synthesis (*ags*) are likely to be located in the T_R-DNA, since this is where the homology to the Ti plasmid *ags* genes is located (17). Recent evidence suggests that at least portions of the Ri T_R-DNA are present in regenerated transformed carrot plants (10). A single T-DNA region has been reported for the mannopine type Ri plasmid (6). Homology data suggest that, although mannopine-type T-DNA shares regions of homology with agropine type T_L-DNA, the two T-DNA regions, and the entire plasmids are quite different (24).

Plants that are regenerated from *A. rhizogenes* infections often have distinct root, flower, stem, and leaf morphological phenotypes (36). The morphological variations may be attributable to the genes of either T-DNA region. The presence and expression of the *tms* genes in differentiated plants is likely to affect root (19) and shoot (5) morphology. The morphogenic effects of the T_L-DNA were visibly apparent only with inoculations on *K. diagremontiana*. However, expression of the T_L-DNA genes may cause morphogenic abnormalities in regenerated plants that are not detectable in stem or leaf tumors. The loss of morphological variations in regenerated plants due to mutations in the T_L-DNA would not have been detected in the virulence assays performed in this study. In fact, preliminary evidence suggests that some features of regenerated plants are due to the presence and expression of genes in the Ri T_L-DNA (B. H. Taylor and F. F. White, unpublished results).

The genes of the Ri T_L-DNA and several genes in the Ti plasmid T-DNA regions have phenotypic effects on tumorigenesis, but have yet to be identified with biochemical functions. The Ri plasmid T_L-DNA is necessary for tumorigenesis on *K. diagremontiana* leaves, a phenotype which is also associated with the *tmr* gene of Ti plasmids. Strains with T_L-DNA deletions behave strikingly similarly to Ti plasmid *tmr* mutants on *K. diagremontiana* stems and leaves. In addition, the loss of virulence symptoms on *K. diagremontiana* leaves by a *tmr* mutation can be restored by the introduction of the Ri plasmid T_L-DNA region. By analogy to *tmr*, which is involved in the biosynthetic pathway for cytokinin (1, 3), the genes of the T_L-DNA may be involved in the synthesis or regulation of substances with cytokinin-like effects. Although cytokinins are known to inhibit root development, these results suggest that either a particular type of cytokinin or low levels of cytokinin may stimulate root development. The stimulation of lateral root formation by low levels of exogenously supplied cytokinins has been reported (37, 43).

Biochemical analysis of the alterations in the levels of phytohormones of plants transformed with pRiA4b is the next step toward an understanding of hairy root tumorigenesis. Correlation of the mutations in the Ri plasmid T-DNA and changes in the biochemical events of the plant also promises to provide considerable insight into the normal process of plant root development.

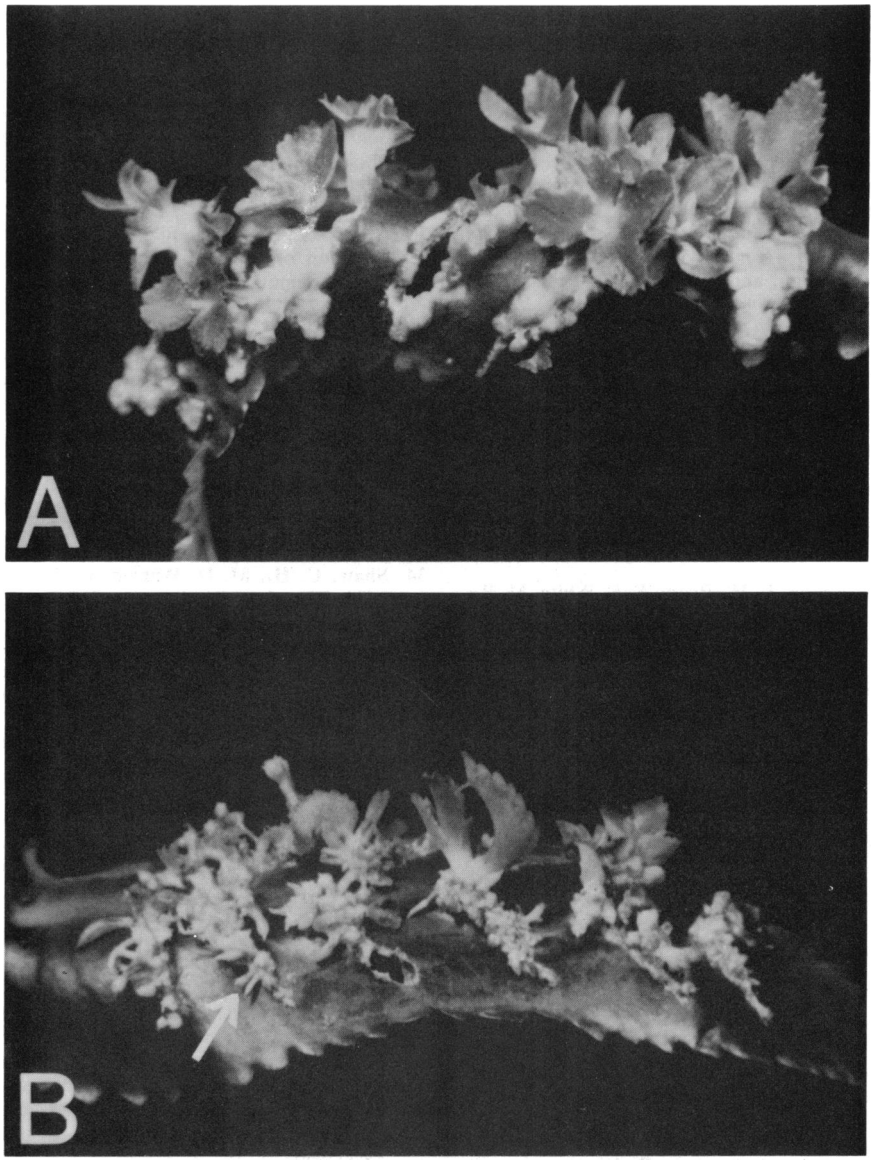

FIG. 8. Insertion of the pTiA6NC *tmr* locus into pRiA4b. Tumors 2 months after inoculation of *K. diagremontiana* leaves with (A) R1236 (pRiA4b with insertion of *tmr* and deletion of T_L-DNA); (B) R1235 (wild-type pRiA4b with insertion of *tmr*). Note the presence of roots in inoculations of leaves with R1235 (arrow) and the absence of roots in inoculations with R1236.

ACKNOWLEDGMENTS

Expert technical assistance was provided by Lin-Sec Wong. Additional assistance with plant materials was provided by Gina Stuart and Brian Watson. We thank Sharon Bradley for final preparation of the manuscript and I. Furner, H. Klee, M. Yanofsky, and S. Ziegler for helpful criticisms.

F.F.W. was supported by a National Science Foundation Postdoctoral Fellowship and by an award from the Standard Oil of Indiana Corp. B.H.T. was supported by a National Science Foundation Predoctoral Fellowship. G.A.H. was supported by Public Health Service grant CA-07017 from the National Cancer Institute.

LITERATURE CITED

1. **Akiyoshi, D. E., H. J. Klee, R. Amasino, E. W. Nester, and M. P. Gordon.** 1984. T-DNA of *Agrobacterium tumefaciens* codes an enzyme of cytokinin biosynthesis. Proc. Natl. Acad. Sci. USA **81**:5994–5998.
2. **Akiyoshi, D. E., R. O. Morris, R. Hinz, B. S. Mischke, T. Kosuge, D. J. Garfinkel, M. P. Gordon, and E. W. Nester.** 1983. Cytokinin/auxin balance in crown gall tumors is regulated by specific loci in the T-DNA. Proc. Natl. Acad. Sci. USA **80**:407–441.
3. **Barry, G. F., S. G. Rogers, R. T. Fraley, and L. Brand.** 1984. Identification of a cloned cytokinin biosynthetic gene. Proc. Natl. Acad. Sci. USA **81**:4776–4780.
4. **Birnboim, H. C., and J. Doly.** 1979. A rapid alkaline extraction procedure for screening recombinant plasmid DNA. Nucleic Acids Res. **7**:1513–1523.
5. **Buchholz, W. G., and M. F. Thomashow.** 1984. Comparison of T-DNA oncogene complements of *Agrobacterium tumefaciens* tumor-inducing plasmids with limited and wide host ranges. J. Bacteriol. **160**:319–326.
6. **Byrne, M. C., J. Koplow, C. David, J. Tempe, and M.-D. Chilton.** 1983. Structure of T-DNA in roots transformed by *Agrobacterium rhizogenes*. J. Mol. Appl. Genet. **2**:201–209.
7. **Chilton, M.-D., T. C. Currier, S. K. Farrand, A. J. Bendich, M. P. Gordon, and E. W. Nester.** 1974. *Agrobacterium tumefaciens* DNA and PS8 bacteriophage DNA not detected in crown gall tumors. Proc. Natl. Acad. Sci. USA **71**:3672–3676.
8. **Costantino, P., M. L. Mauro, G. Mitcheli, G. Risuleo, P. J. J.**

Hooykaas, and R. A. Schilperoort. 1981. Fingerprinting and sequence homology of plasmids from different virulent strains of *Agrobacterium rhizogenes*. Plasmid **5**:170–182.

9. **Costantino, P., L. Spano, M. Pomponi, E. Benvenuto, and G. Ancora.** 1984. The T-DNA of *Agrobacterium rhizogenes* is transmitted through meiosis to the progeny of hairy root plants. J. Mol. Appl. Genet. **2**:465–470.
10. **DePaolis, A., M. L. Mauro, M. Pomponi, M. Cardarelli, L. Spano, and P. Costantino.** 1985. Localization of agropine-synthesizing functions in the T_R region of the root-inducing plasmid of *Agrobacterium rhizogenes* 1855. Plasmid **13**:1–17.
11. **Depicker, A., M. Van Montagu, and J. Schell.** 1983. Plant cell transformation by *Agrobacterium* plasmids, p. 499. *In* T. Kosuge, C. P. Meredith, and A. Hollaender (ed.), Genetic engineering of plants: an agricultural perspective. Plenum Publishing Corp., New York.
12. **Ditta, G., S. Stanfield, D. Corbin, and D. R. Helinski.** 1981. Broad host range DNA cloning system for gram-negative bacteria: construction of a gene bank of *Rhizobium meliloti*. Proc. Natl. Acad. Sci. USA **77**:7347–7351.
13. **Galbraith, D. W., K. R. Harkins, J. M. Maddox, N. M. Ayres, D. P. Sharma, and E. Firoozabady.** 1983. Rapid flow cytometric analysis of the cell cycle in intact plant tissues. Science **220**:1049–1051.
14. **Garfinkel, D. J., R. B. Simpson, L. W. Ream, F. F. White, M. P. Gordon, and E. W. Nester.** 1981. Genetic analysis of crown gall: fine structure map of the T-DNA by site-directed mutagenesis. Cell **27**:143–153.
15. **Hohn, B., and J. Collins.** 1980. A small cosmid for efficient cloning of large DNA fragments. Gene **11**:218–225.
16. **Holsters, M., D. de Waele, A. Depicker, E. Messens, M. Van Montagu, and J. Schell.** 1978. Transfection and transformation of *Agrobacterium tumefaciens*. Mol. Gen. Genet. **163**:181–187.
17. **Huffman, G. A., F. F. White, M. P. Gordon, and E. W. Nester.** 1984. Hairy-root-inducing plasmid: physical map and homology to tumor-inducing plasmids. J. Bacteriol. **157**:269–276.
18. **Inze, D., A. Follin, M. Van Lijsebettins, C. Simoens, C. Genetello, M. Van Montagu, and J. Schell.** 1984. Genetic analysis of the individual T-DNA genes of *Agrobacterium tumefaciens*; further evidence that two genes are involved in indole-3-acetic acid synthesis. Mol. Gen. Genet. **194**:265–274.
19. **Joos, H., D. Inze, A. Caplan, M. Sormann, M. Van Montagu, and J. Schell.** 1983. Genetic analysis of T-DNA transcripts in nopaline crown galls. Cell **32**:1057–1067.
20. **Jorgenson, R. A., S. Rothstein, and W. S. Reznikoff.** 1979. A restriction enzyme cleavage map of Tn*5* and location of a region encoding neomycin resistance. Mol. Gen. Genet. **177**:65–72.
21. **Klee, H., A. Montoya, F. Hordyski, C. Lichtenstein, D. Garfinkel, S. Fuller, C. Flores, J. Peschon, E. W. Nester, and M. P. Gordon.** 1984. Nucleotide sequence of the *tms* genes of the pTiA6NC octopine Ti-plasmid: Two gene products involved in plant tumorigenesis. Proc. Natl. Acad. Sci. USA **81**:1728–1732.
22. **Knauf, V. C., and E. W. Nester.** 1982. Wide host range cloning vectors: a cosmid clone bank of an *Agrobacterium* Ti plasmid. Plasmid **8**:45–54.
23. **Koekman, B. P., G. Ooms, P. M. Klapwijk, and R. A. Schilperoort.** 1979. Genetic map of an octopine Ti-plasmid. Plasmid **2**:347–357.
24. **Lahners, K., M. C. Byrne, and M.-D. Chilton.** 1984. T-DNA fragments of hairy root plasmid pRi8196 are distantly related to octopine and nopaline Ti plasmid T-DNA. Plasmid **11**:130–140.
25. **Leong, S. A., G. S. Ditta, and D. R. Helinski.** 1982. Heme biosynthesis in *Rhizobium*: identification of a cloned gene coding for δ-aminolevulinic acid synthase from *Rhizobium meliloti*. J. Biol. Chem. **257**:8724–8730.
26. **Moore, L., G. Warren, and G. Strobel.** 1979. Involvement of a plasmid in the hairy root disease of plants caused by *Agrobacterium rhizogenes*. Plasmid **2**:617–626.
27. **Murray, G. M., and W. F. Thompson.** 1980. Rapid isolation of high molecular weight plant DNA. Nucleic Acids Res. **8**: 4321–4325.
28. **Nester, E. W., M. P. Gordon, R. M. Amasino, and M. F. Yanofsky.** 1984. Crown gall: a molecular and physiological analysis. Annu. Rev. Plant Physiol. **35**:387–413.
29. **Ooms, G., P. J. J. Hooykaas, G. Moolenaar, and R. A. Schilperoort.** 1981. Crown gall plant tumors of abnormal morphology, induced by *Agrobacterium tumefaciens* carrying mutated octopine Ti-plasmids; analysis of T-DNA functions. Gene **14**:33–50.
30. **Ooms, G., L. Molendijk, and R. Schilperoort.** 1982. Double infection of tobacco plants by two complementing octopine T-region mutants of *Agrobacterium tumefaciens*. Plant Mol. Biol. **1**:217–226.
31. **Petit, A., C. David, G. A. Dahl, J. G. Ellis, P. Guyon, F. Casse-Delbart, and J. Tempe.** 1983. Further extension of the opine concept: plasmids in *Agrobacterium rhizogenes* cooperate for opine degradation. Mol. Gen. Genet. **190**:204–214.
32. **Ruvkun, G. B., and F. M. Ausubel.** 1981. A general method for site-directed mutagenesis in prokaryotes. Nature (London) **289**:85–88.
33. **Schroder, G., S. Waffenschmidt, E. W. Weiler, and J. Schoder.** 1984. The T-region of Ti plasmids codes for an enzyme synthesizing indole-3-acetic acid. Eur. J. Biochem. **138**:387–391.
34. **Shaw, C. H., M. D. Watson, G. H. Carter, and C. H. Shaw.** 1984. The right hand copy of the nopaline Ti-plasmid 25 bp repeat is required for tumour formation. Nucleic Acids Res. **12**:6031–6041.
35. **Southern, E. M.** 1975. Detection of specific sequences among DNA fragments separated by gel electrophoresis. J. Mol. Biol. **98**:503–517.

35a. **Stachel, S. E., G. An, C. Flores, and E. W. Nester.** 1985. A Tn*3* *lac-2* transposon for the random generation of β-galactosidase gene fusions: application to the analysis of gene expression in *Agrobacterium*. EMBO J. **4**:891–898.

36. **Tepfer, D.** 1984. Transformation of several species of higher plants by *Agrobacterium rhizogenes*: sexual transmission of the transformed genotype and phenotype. Cell **37**:959–967.
37. **Torrey, J. G.** 1962. Auxin and purine interactions in lateral root initiation in isolated pea root segments. Physiol. Plant **15**:177–185.
38. **Vieira, J., and J. Messing.** 1982. The pUC plasmids, an M13mp7-derived system for insertion mutagenesis and sequencing with synthetic universal primers. Gene **19**:259–268.
39. **Wang, K., L. Herrera-Estrella, M. Van Montagu, and P. Zambryski.** 1984. Right 25-bp terminus sequence of the nopaline T-DNA is essential for and determines direction of DNA transfer from *Agrobacterium* to the plant genome. Cell **38**:455–462.
40. **White, F. F., D. J. Garfinkel, G. A. Huffman, M. P. Gordon, and E. W. Nester.** 1983. Sequences homologous to *Agrobacterium rhizogenes* T-DNA in the genomes of uninfected plants. Nature (London) **301**:348–350.
41. **White, F. F., and E. W. Nester.** 1980. Hairy root: plasmid encodes virulence traits in *Agrobacterium rhizogenes*. J. Bacteriol. **141**:1134–1141.
42. **White, F. F., and E. W. Nester.** 1980. Relationship of plasmids responsible for hairy root and crown gall tumorigenicity. J. Bacteriol. **144**:710–720.
43. **Wightman, F., E. A. Schneider, and F. V. Thimann.** 1980. Hormonal factors controlling the initiation and development of lateral roots. II. Effects of exogenous growth factors on lateral root formation in pea roots. Physiol. Plant **49**:304–414.
44. **Willmitzer, L., J. Sanchez-Serrano, E. Buschfeld, and J. Schell.** 1982. DNA from *Agrobacterium rhizogenes* is transferred to and expressed in axenic hairy root plant tissues. Mol. Gen. Genet. **186**:16–22.
45. **Yanofsky, M., A. Montoya, V. Knauf, B. Lowe, M. Gordon, and E. Nester.** 1985. Limited-host-range plasmid of *Agrobacterium tumefaciens*: molecular and genetic analyses of transferred DNA. J. Bacteriol. **163**:341–348.